such an orientation leads to the equatorial alcohol (Scheme I). Such intermediates also neatly explain the isomerizations from *cis*- to *trans*-2-vinylcyclobutanols observed here as well as in related systems in our earlier report and in the example reported by Gadwood.[4] The same hypothesis readily explains why **13** ($R = H$) undergoes the [1,3] shift to a ring-expanded product whereas **13** ($R = CH_3$) undergoes ring opening to **15**;[5] the intermediate anion ketone **14** can easily undergo a 1,5-proton transfer to yield the enolate precursor of **15**. This may also be the explanation for the sharply reduced yields of ring-expansion product noted by Danheiser when an alkyl group was present on the carbinol carbon atom of the cyclobutanol.[3]

Acknowledgments. We thank Professors Kendall N. Houk and Nelson G. Rondan for stimulating discussions, Dr. Alvin Marcus for recording the mass spectra, the National Institutes of Health for providing financial support (GM 22760), and the National Science Foundation for funds used to purchase the 300-MHz Bruker NMR instrument used in this study (CHE 7905185).

Anion-Assisted Transfer of a Sterically Constrained Proton: Molecular Structure of $HMo(CO)_2(Ph_2PCH_2CH_2PPh_2)_2^+ AlCl_4^-$

John M. Hanckel and Marcetta Y. Darensbourg*

Department of Chemistry, Texas A&M University
College Station, Texas 77843

Received July 8, 1983

The understanding of heterolytic activation of dihydrogen by transition-metal catalysts requires knowledge of $M-H^+$ as well as $M-H^-$ bond reactivity. Two recent physical organometallic studies have provided fundamentally important thermodynamic and kinetic stability measurements of the deprotonation of structurally simple neutral metal carbonyl hydrides.[1,2] Jordan and Norton noted that "...knowledge of proton-transfer rates in straightforward cases should help identify less obvious proton-transfer mechanisms."[1] Accordingly reported herein is our study of $HMo(CO)_2(Ph_2P(CH_2)_2PPh_2)_2^+$ (**1H**$^+$),[3,4] which notes unusual and significant counterion influences on proton-transfer reaction rates and equilibrium positions.

Although tetrahydrofuran solutions of **1H**$^+$ BF_4^- were observed to be stable for several days at room temperature, the $AlCl_4^-$ salt deprotonated significantly in less than 24 h, producing *cis*-$Mo(CO)_2(DPPE)_2$ (*cis*-**1**). Since chloride is known to be readily displaced from $AlCl_4^-$ (and even $AlCl_3$) by THF[5] but BF_4^- is stable even in water, the role of chloride anion in the deprotonation of **1H**$^+$ was implicated. The following study was designed to define the system.

Reactions of **1H**$^+$ BF_4^- with a variety of different bases and base mixtures (eq 1) in CH_2Cl_2 were monitored to equilibrium by

$$HMo(CO)_2(DPPE)_2^+ BF_4^- + \text{base} \underset{k_{-1}}{\overset{k_1}{\rightleftharpoons}} Mo(CO)_2(DPPE)_2 + \text{base}{\cdot}H^+ BF_4^- \quad (1)$$

FT-IR.[7] The data in Table I infer a qualitative and typical ordering of base strengths: $F^- \sim OAc^- > NEt_3 > NHEt_2 > py > Cl^- > I^-$.

Table I. Deprotonation Reactions of $[HMo(CO)_2(DPPE)_2^+] BF_4^-$ (0.0040 M in CH_2Cl_2 Solution): Equilibrium Positions

base	equiv	% deprotonation at equilibrium (time)
pyridine	25	45 (5 d)
$NHEt_2$	25	75 (10 d)
NEt_3	25	100 (3 d)
PPN^+Cl^-	25	20 (4-6 h)
PPN^+OAc^-	10	100 (4-6 h)
PPN^+OAc^-	2	95 (18 h)
PPN^+I^-	25	10 (4-6 h)
PPN^+F^-	10	100 (1 h)
PPN^+F^-	2	95 (18 h)

Whereas the equilibrium data of Table I provided no surprises, the rates of reaching equilibrium did not correlate with thermodynamic base strengths. The rate of reaction 1 using pyridine as base showed a first-order dependence both on [**1H**$^+$] and on [py] (Table II). Addition of $PPN^+ Cl^-$ to the reaction of **1H**$^+$ and pyridine resulted in 100% deprotonation and a rate enhancement of ca. 10^2. As noted in Table II, the pseudo-first-order rate constants of chloride/pyridine mixtures were linearly dependent on [Cl^-] but *independent* of [py] or of the amine itself (i.e., NEt_3, entry 9). Thus the sole function of the amine is to serve as a thermodynamic trap for HCl.

Deprotonation rates in the presence of other anionic additives (Table II) vary in the order $F^- > Cl^- > OAc^- > I^-$. The reactivity order for the halides compares favorably with their order to thermodynamic base strengths. However pyridine and acetate are both stronger bases than Cl^- but in reaction 1 are kinetically less reactive. Consistent with this apparent dependence of kinetic reactivity on the size of the deprotonating agent 2,6-lutidene does not react with **1H**$^+$ BF_4^- over a period of days.

An equally impressive counterion effect was observed for the rate of proton exchange between **1** and ^{13}CO-labeled **1H**$^+$ (eq 2).[9]

$$\underset{^{13}\mathbf{1H}^+}{HMo(^{13}CO)_2(DPPE)_2^+ BF_4^-} + \underset{^{12}\mathbf{1}}{Mo(^{12}CO)_2(DPPE)_2} \xrightleftharpoons{CH_2Cl_2} \underset{^{12}\mathbf{1H}^+}{HMo(^{12}CO)_2(DPPE)_2^+ BF_4^-} + \underset{^{13}\mathbf{1}}{Mo(^{13}CO)_2(DPPE)_2} \quad (2)$$

In the absence of any additives reaction 2 failed to produce any exchange products within 24 h; however addition of 0.5 equiv of $PPN^+ Cl^-$ produced the expected statistical ratio of $^{13}\mathbf{1}/^{12}\mathbf{1}$ within 6 h. There was no intermolecular CO exchange within 24 h. Few examples of such slow rates of proton-exchange reactions have been reported. At least one example is provided in J.-M. Lehn's cryptand chemistry, but it is an example of a protonated site severely constrained both electronically and sterically in the interior of a large cryptand.[10]

The implication of steric constraints on deprotonation is substantiated by the molecular structure of $HMo(CO)_2(DPPE)_2^+$-$AlCl_4^-$ as determined by single-crystal X-ray diffraction analysis.[11]

---

(1) Jordan, R. F.; Norton, J. R. *J. Am. Chem. Soc.* **1982**, *104*, 1255.

(2) Walker, H. W.; Pearson, R. G.; Ford, P. C. *J. Am. Chem. Soc.* **1983**, *105*, 1179.

(3) Datta, S.; Dezube, B.; Kouba, J. K.; Wreford, S. S. *J. Am. Chem. Soc.* **1978**, *100*, 4404.

(4) Datta, S.; McNeese, T. J.; Wreford, S. S. *Inorg. Chem.* **1977**, *16*, 2661.

(5) Derouault, J.; Granger, P.; Ford, M. T. *Inorg. Chem.* **1977**, *16*, 3214.

(6) Massey, A. G. *Adv. Inorg. Chem. Radiochem.* **1967**, *10*, 99.

(7) Pertinent ν(CO) band positions in CH_2Cl_2: $HMo(CO)_2(DPPE)_2^+$, 1880 cm^{-1}; *cis*-$Mo(CO)_2(DPPE)_2$, 1851 s, 1781 s; *trans*-$Mo(CO)_2(DPPE)_2$, 1822 s.

(8) All kinetic studies were performed in CH_2Cl_2 and reactions were followed by observation of the 1880-cm^{-1} band of **1H**$^+$. Values of k_{obsd} were determined from pseudo-first-order plots of ln (Abs − Abs$_\infty$) vs. time. Abs$_\infty$ represents an equilibrium value for entries 1-4 (Table II). Reactions 5-13 resulted in 100% deprotonation.

(9) $Mo(^{13}CO)_2(DPPE)_2$ was prepared as described in ref 3. $HMo(^{13}CO)_2(DPPE)_2BF_4$ was prepared by reaction of $Mo(^{13}CO)_2(DPPE)_2$ with $HBF_4{\cdot}OEt_2$ in THF. ν(CO) IR band positions in CH_2Cl_2: *cis*-$Mo(^{13}CO)_2(DPPE)_2$, 1808 s, 1742 s; *trans*-$Mo(^{13}CO)_2(DPPE)_2$, 1782 s; *trans*-$HMo(^{13}CO)_2(DPPE)_2^+$, 1839 cm^{-1}.

(10) Smith, P. B.; Dye, J. L.; Cheney, J.; Lehn, J.-M. *J. Am. Chem. Soc.*, **1982**, *103*, 6044.

(11) Single crystals of **1H**$^+$ $AlCl_4^-$ were grown from THF/hexane and data collection carried out at 23 °C. The compound is in the monoclinic space group *Cc* with $a = 16.897$ (4) Å, $b = 15.573$ (5) Å, $c = 23.501$ (13) Å; $\beta = 91.55$ (3)°; $Z = 4$. $R_W = 0.054$ for 4675 reflections with $I > 3\sigma(I)$. Crystallographic analysis was carried out by Molecular Structure Corporation, College Station, TX. Details to be published separately.

0002-7863/83/1505-6979$01.50/0

Table II. Rates of Deprotonation of $HMo(CO)_2(DPPE)_2^+ BF_4^-$ (0.004 M in CH_2Cl_2) by Pyridine and Pyridine in the Presence of Additives

entry	[py], M	equiv	anion[a]	[anion], M	equiv	k_{obsd}, min^{-1} [b]	k_1, min^{-1} M^{-1} [c]
1	0.10	25				$4.14 (\pm 0.38) \times 10^{-4}$	4.14×10^{-3}
2	0.18	35				$6.57 (\pm 0.22) \times 10^{-4}$	3.65×10^{-3}
3	0.22	45				$7.78 (\pm 0.26) \times 10^{-4}$	3.53×10^{-3}
4	0.26	55				$9.22 (\pm 0.39) \times 10^{-4}$	3.55×10^{-3}
5	0.060	20	Cl^-	0.060	15	$1.18 (\pm 0.11) \times 10^{-2}$	1.96×10^{-1}
6	0.080	20	Cl^-	0.088	22	$1.70 (\pm 0.18) \times 10^{-2}$	1.93×10^{-1}
7	0.080	20	Cl^-	0.120	30	$2.38 (\pm 0.10) \times 10^{-2}$	1.98×10^{-1}
8	0.020	5	Cl^-	0.080	20	$1.65 (\pm 0.07) \times 10^{-2}$	2.06×10^{-1}
9[d]	0.080 (NEt_3)	20	Cl^-	0.080	20	$1.61 (\pm 0.007) \times 10^{-2}$	2.01×10^{-1}
10	0.080	20	OAc^-	0.080	20	$1.00 (\pm 0.002) \times 10^{-2}$	1.21×10^{-1}
11[e]	0.080	20	OAc^-	0.068	17	$7.56 (\pm 0.15) \times 10^{-3}$	1.10×10^{-1}
12	0.080	20	I^-	0.080	20	$1.12 (\pm 0.13) \times 10^{-3}$	1.40×10^{-2}
13	0.080	20	F^-	0.080	20	too rapid to measure	

[a] Added salts have the bis(triphenylphosphine)imminium, PPN^+, counterion except where indicated. [b] Obtained by a plot of ln ($Abs_t - Abs_\infty$) vs. time over 1–2 half-lives of reaction. Error calculated at 95% confidence limit for an individual run. Reproducibility was within 5–10%. [c] Obtained by k_{obsd}/[py] for entries 1–4 and by k_{obsd}/[anion] for entries 5–12. k_1 is the second-order rate constant defined by eq 1. [d] In this run NEt_3 was used as base instead of pyridine. [e] Acetate added as the $K^+ \cdot$benzo-18-C-6 salt.

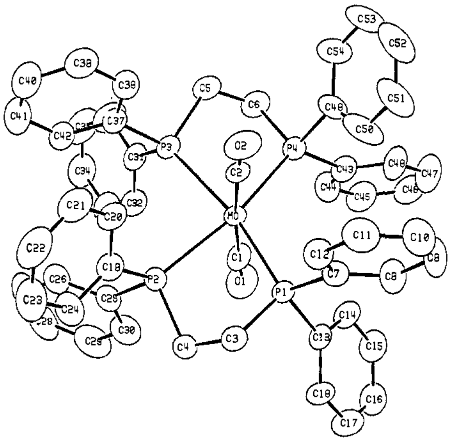

Figure 1. An ORTEP drawing of $HMo(CO)_2(DPPE)_2^+$ showing 40% probability ellipsoids. Phenyl hydrogen atoms were included in calculated positions (assuming idealized geometries with C–H = 0.95 Å) and were not refined. Pertinent bond lengths and bond angles: Mo–P1, 2.466 (1); Mo–P2, 2.574 (2); Mo–P3, 2.583 (2); Mo–P4, 2.468 (2); Mo–C1, 2.021 (8); Mo–C2, 1.900 (8) Å. P1–Mo–P4, 114.61(6)°; P2–Mo–P3, 89.62 (6)°; P3–Mo–P4, 78.28 (6)°; P1–Mo–P2, 77.8 (6)°; C1–Mo–C2, 175.4 (3)°

The ORTEP plot in Figure 1 shows the structure of the cation to be one with a trans arrangement of CO groups and the P-donor atoms to be roughly in a plane. Although refined to a (weighted) agreement factor of 0.054, the hydride was not observed in the final difference map. On examination of the MoP_4 bond angles and distances and by comparison to the structures of $HTa(CCMe_3)(Me_2PCH_2CH_2PMe_2)_2(ClAlMe_3)$[12] and $HTa(CO)_2(Me_2PCH_2CH_2PMe_2)_2$,[13] the hydride position is inferred to be between P1 and P4, in or very near the MoP_4 plane. To our knowledge this is the first example of two DPPE ligands occupying the plane of a PB structure.[14]

We have thus implicated a simple mechanism for deprotonation in which bases burrow into the $Mo-H^+$ binding site, electrostatically interact with the proton, and abstract it. There are, however, in the cationic complex additional sites for nucleophilic attack: the carbonyl carbon and the molybdenum(II) center. Base or anion interaction at these sites might reasonably be proposed to precede H^+ abstraction. Nevertheless there was found no spectroscopic evidence for formation of adducts of any type,[15] and furthermore no easy way to explain why either of the two alternate reaction (or prereaction) sites might show the observed dependence of rate on anion size.

Acknowledgment. Appreciation is expressed to the Robert A. Welch Foundation and to the National Science Foundation for support of this work.

---

(12) Churchill, M. R.; Wasserman, H. J.; Turner, H. W.; Shrock, R. R. *J. Am. Chem. Soc.* **1982**, *104*, 1710.

(13) Meakin, P.; Guggenberger, L. J.; Tebbe, F. N.; Jesson, J. P. *Inorg. Chem.* **1974**, *13*, 1025.

(14) Drew, M. G. B. *Prog. Inorg. Chem.* **1977**, *23*, 67.

(15) Angelici, R. *J. Acc. Chem. Res.* **1972**, *5*, 335.

Ethylene and Acetylene Complexes of the Silver Atom

Drora Cohen and Harold Basch*

Department of Chemistry, Bar Ilan University
Ramat-Gan 52100, Israel

Received June 20, 1983

Recently reported low-temperature matrix-isolation ESR studies of the mono- and diacetylene and ethylene complexes of copper and silver atoms have led to the unexpected conclusion that the electronic ground states of the symmetric complexes, where these have been isolated, correlate with the metal atom being in an excited $5p^1(^2P)$ rather than in the ground $5s^1(^2S)$ state.[1,2] In order to quantitatively characterize the geometries of these interesting complexes and gain insight into their electronic structure, we have carried out ab initio self-consistent-field (SCF) calculations on $Ag(C_2H_4)_{1,2}$ and $Ag(C_2H_2)_{1,2}$ using a relativistic effective core potential (RECP)[3,4] for the silver atom and gradient optimization techniques[5] for the geometries.

Restricted open- or closed-shell SCF calculations were carried out on all the systems studied here using the $[3^s2^p/2^s]$ contracted basis described by Dunning and Hay[6] for the carbon/hydrogen atoms. The calculated optimum geometries for C_2H_4 and C_2H_2 in this basis are very close to their respective experimental values, as can be seen from Table I where the optimized geometries are described. For the silver atom the $[3^s2^p2^d]$ valence basis and RECP were taken from previous studies of Ag atom clusters.[3,4]

For the diligand complexes only the symmetric D_{2h} geometry was investigated, where the ligands adopt an eclipsed parallel conformation, one on each side of the silver atom. If the plane containing the Ag and four carbon atoms is defined as XY with Y parallel to, and X bisecting, the C–C bonds, then the four electronic states arising out of the limiting silver atom ^2S and ^2P

---

(1) Kasai, P. H.; McLeod, D., Jr.; Watanabe, T. *J. Am. Chem. Soc.* **1980**, *102*, 179.

(2) Kasai, P. H. *J. Phys. Chem.* **1982**, *86*, 3684.

(3) Basch, H. *J. Am. Chem. Soc.* **1981**, *103*, 7863.

(4) Basch, H. *Symp. Faraday Soc.* **1980**, *No.* **14**, 149.

(5) The program GAMESS (M. Dupuis, private communication) was modified to include effective core potentials in the gradient-optimization procedure.

(6) Dunning, T. H.; Hay, P. J. In "Modern Theoretical Chemistry III. Methods of Electronic Structure Theory"; Schafer, H. F., III, Ed.; Plenum Press: New York, 1977; H. F.; Schaefer III, Ed., p 1.

0002-7863/83/1505-6980$01.50/0 © 1983 American Chemical Society